NOTE

The Tuning Fork Artifact in Computerized Tomography

L. A. SHEPP

Bell Laboratories, Murray Hill, New Jersey 07974

AND

S. K. HILAL AND R. A. SCHULZ

*The Neurological Institute, Columbia Presbyterian Medical Center,
New York, New York 10032*

It is apparently well known that one particularly delicate tolerance in designing a tomographic machine is that on the error in alignment of the graticule. If the graticule, or strip which determines the location of the parallel measurements in each view, is displaced by as little as 0.05 mm consistently in each view, a characteristic artifact resembling a tuning fork can appear in the neighborhood of a small dense object (e.g., the petrous bone). In this paper, we give a mathematical analysis of this artifact, leading to a simple quantitative estimate of this error in terms of the displacement. We also show that a rough correction can easily be made in software to remove this artifact by making the opposite shift in the weight function used. We show further that the displacement can be indirectly measured by using a pin phantom. Finally, we note that if the displacement were measured directly using, e.g., a triangular piece of lead, the above correction would then remove the artifact and eliminate the need for such a delicate tolerance.

1. INTRODUCTION

In computerized tomography, a density $f(x, y)$ is reconstructed as in [1] from the integrals $P(t, \theta)$ (see [1]) of f along the line with equation $x \cos \theta + y \times \sin \theta = t$, obtained from X-ray measurements. In measuring $P(t, \theta)$, errors occur and produce characteristic artifacts, some of which were studied in [2]. Relative motion of the object with respect to the X-ray beam during the measurement period produces an artifact sometimes called the "patient motion artifact," Fig. 1. A similar artifact occurs in Fig. 2 where the object is a 0.25-in.-diameter aluminum pin and where a vertical strip or tuning fork artifact is seen. This effect is known to be due to the relative motion which occurs when, after each rotating step, the graticule or timing strip (which defines the translation location of the beam) comes to a new position, slightly jittered. The center of rotation should project onto the center point on the graticule in each view, but, because
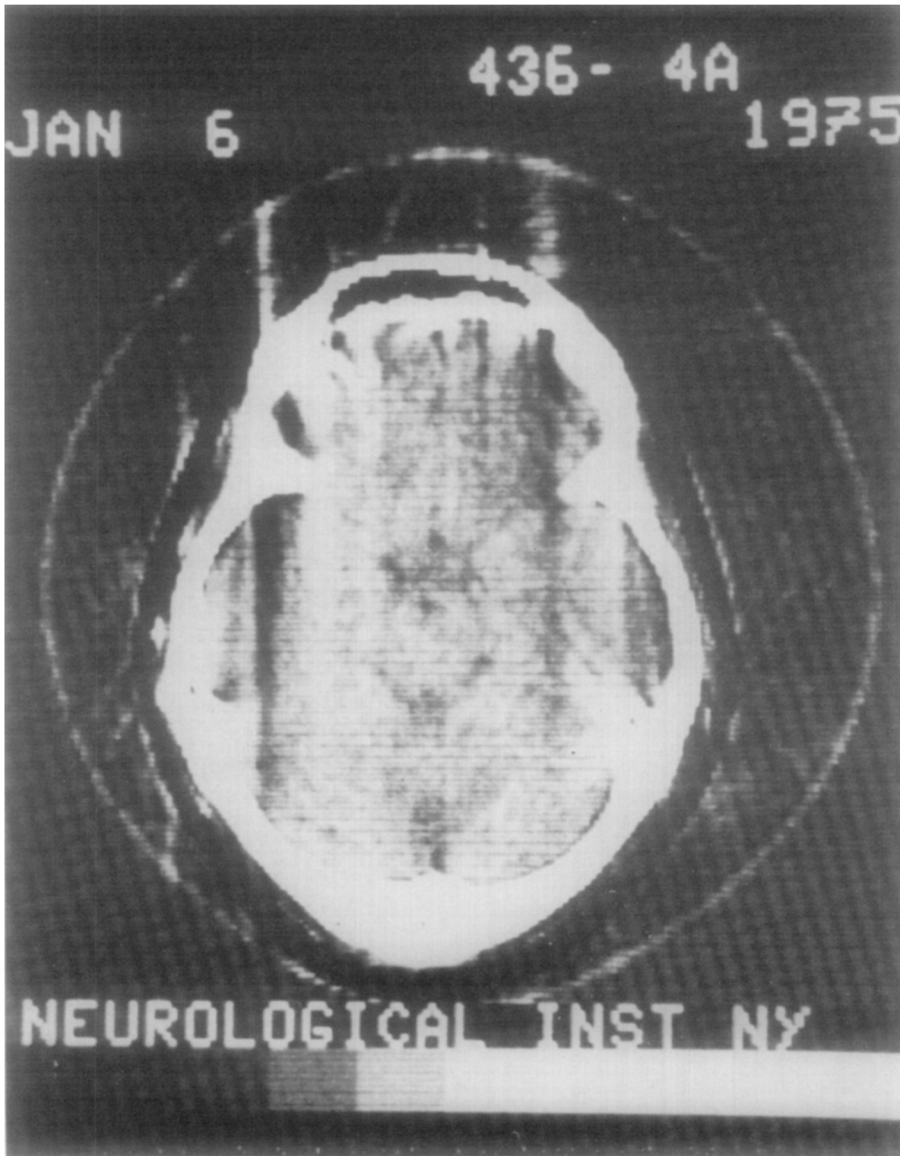
FIG. 1. Reconstruction of a head section (at the level of the midbrain) showing the tuning fork artifact. The artiface emanates from the left frontal bone. There is a dark streak running downward into the brain and a light streak running upward into the water surrounding the head.

of the mechanical jitter, it is shifted by an amount $\delta(\theta)$, causing each ray in the view at angle θ to be shifted parallel to itself by $\delta(\theta)$, so that

$$P^*(t, \theta) = P(t - \delta(\theta), \theta) \tag{1}$$

is the incorrectly measured value of $P(t, \theta)$. In case $\delta(\theta) \equiv \delta$ independent of θ, it is known [3, 4] that a consistent displacement of $\delta = 0.05$ mm of the graticule is
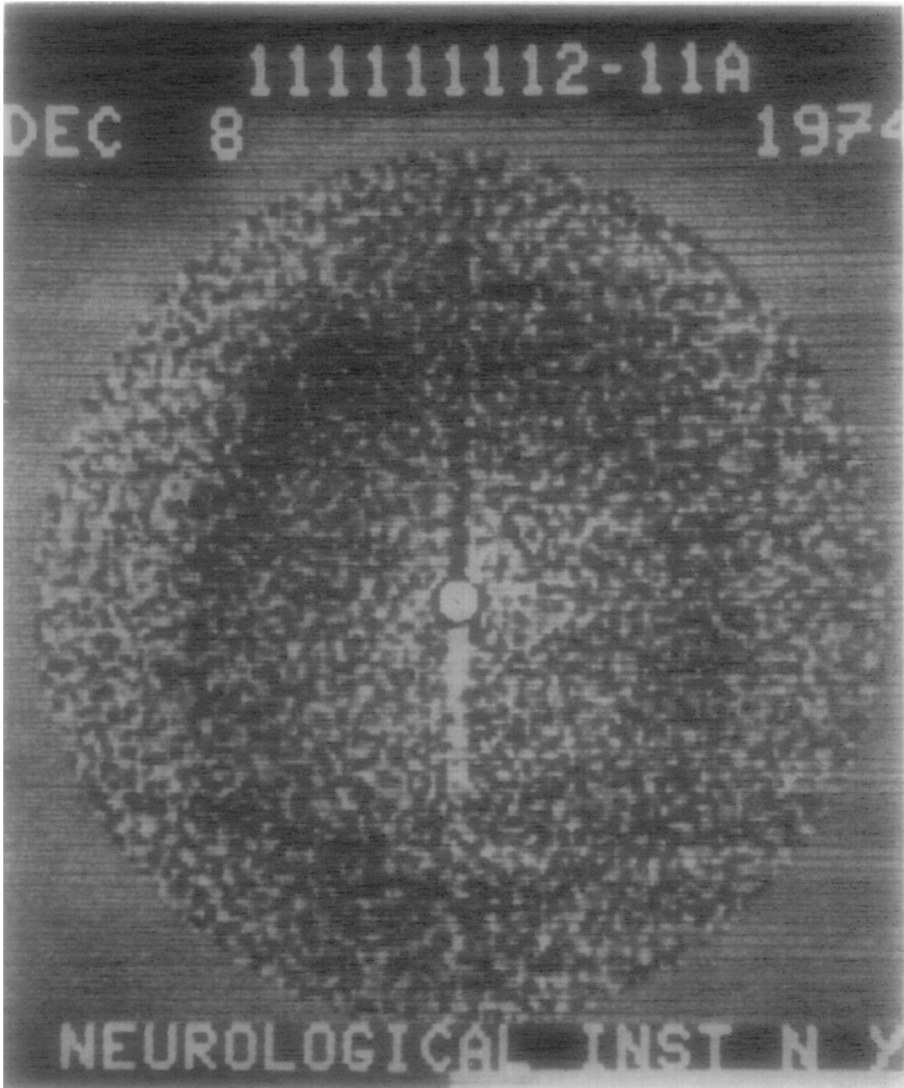
Fɪɢ. 2. Reconstruction of a 0.25-in.-diameter aluminum pin showing the tuning fork artifact. The black at the center of the pin is also an artifact, perhaps due to numerical overload in the display, the pin being unexpectedly dense. This corresponds to Run 1A of Table 1.

enough to cause visible artifacts (Fig. 2). How does one estimate $\delta(\theta)$ in actual practice, however?

2. INDIRECT MEASUREMENT OF $\delta(\theta)$

We obtained the projection data for the pin phantom of Fig. 2 from a tomographic transmission scanner. In each of 180 views the 251 projection values were found to be integers less than about 100 in absolute value for all except about eight central rays (the rays numbered 123–130), which have a maximum of
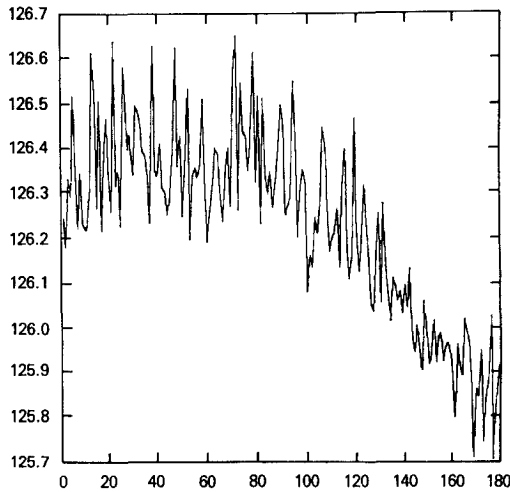
FIG. 3. Plot of estimated projections of the center of the pin onto the graticule as a function of angle 1 to 180°. This corresponds to slice A of run 1 of Table 1.

around 2000, usually at ray 126, the central ray. The center of the pin thus projects somewhere near ray 126 in each view.

In order to determine the projection of the center of the pin onto the graticule more precisely, we fitted a parabola through the largest value of the projection and its two neighbors in each view and took the location c_j of the maximum of
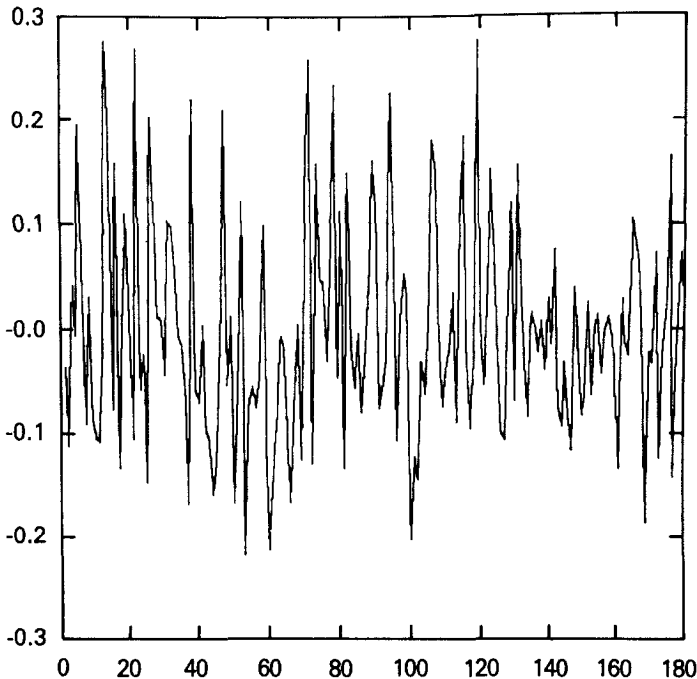

FIG. 4. Residuals of Fig. 3 after a least-squares fit with $x_0 \cos \theta_j + y_0 \sin \theta_j + c$, $x_0 = 0.225$, $y_0 = 0.275$, $c = 126.058$. This corresponds to Run 1A of Table 1.

TABLE 1

Run	Slice	x_0	y_0	δ
1	A	0.225	0.275	0.058
1	B	0.285	0.301	0.057
2	A	0.294	0.195	0.044
2	B	0.347	0.243	0.032
3	A	0.205	0.236	−0.045
3	B	0.264	0.273	−0.045

the parabola as an estimate of the location of the maximum of the projection. We thus took this value c_j (Fig. 3) as the projection of the center of the pin in the jth view, $j = 0, 1, \ldots, 179$. If there were no jitter in centering the jth view the projection of the center of a pin at (x_0, y_0) would be $x_0 \cos \theta_j + y_0 \sin \theta_j$. We thus fitted c_j using least squares with

$$c^*_j = 126 + x_0 \cos \theta_j + y_0 \sin \theta_j + \delta, \tag{2}$$

where $\theta_j = j\pi/180$, $j = 0, 1, \ldots, 179$, and determined the best values of (x_0, y_0) and the average value of δ of the shift $\delta(\theta)$. The residuals $c_j - c^*_j$ are shown in Fig. 4. We obtained the values given in Table 1 for each of two slices A and B for each of three runs. Assuming the distance between adjacent parallel rays in in each view to be about 1 mm, Table 1 indicates that in each slice the center of the pin is at (x_0, y_0), given in mm; in particular, the pin appears to be centered close to the intended center of rotation, i.e., within 1 mm. Further, the average shift δ is about 0.05 mm in each case. Figure 4 indicates the accuracy to which δ can be presumed known; e.g., the standard deviation of the mean of δ is about $0.1/(180)^{\frac{1}{2}} \approx 0.007$ mm. To be more conservative here we should perhaps use $0.1/n^{\frac{1}{2}}$, where $180 > n \approx 30$, because of the evident correlation between points in Fig. 4. We next show that we can remove the artifact by recentering the projections.

3. CORRECTION FOR CENTERING ERROR

If we know the values of $\delta(\theta)$ in (1) it is easy to modify formula (12) of [1] to make the appropriate correction. Using any weight function [1], ϕ, set with $\delta_j = \delta(\theta_j)$, as the corrected reconstruction:

$$f^*_\varphi(x, y) = \frac{a}{2n} \sum_{j=0}^{n-1} \sum_k p^*(t_k, \theta_j)\, \varphi(x \cos \theta_j + y \sin \theta_j - t_k + \delta_j). \tag{3}$$

Since the inner sum is a convolution, the shift (1) in P has been achieved by shifting φ, which is easily implemented in the program.

If δ_j were known precisely (3) should be used, but in our case, since c_j varies wildly (due to noise in the projections), as is clear from Fig. 3, we use only a gross, average correction based on an estimate Δ of the average value of δ_j and set $\delta_j \equiv \Delta$ in (3). In each case this choice removes the artifact. Further, if we vary $\Delta = -0.2, -0.1, -0.05, 0, 0.05, 0.1, 0.2,$ and 0.3 mm, respectively, we

obtain the eight reconstructions, shown from left to right in Fig. 5 for the case of slice B of run 1, which shows that the artifact can be focused out by choosing Δ. A picture essentially identical to Fig. 5 was obtained for slice A of run 1, and corresponding pictures were obtained for the other runs; they were consistent with our explanation in each case.

4. AN APPROXIMATE FORMULA FOR THE ERROR

The error or artifact at height y mm above or below the center (x_0, y_0) of a pin of radius $b \ll |y|$ and density D due to a shift of size δ mm in every ray of every view (the views start and end in the vertical direction as is usual in 180°
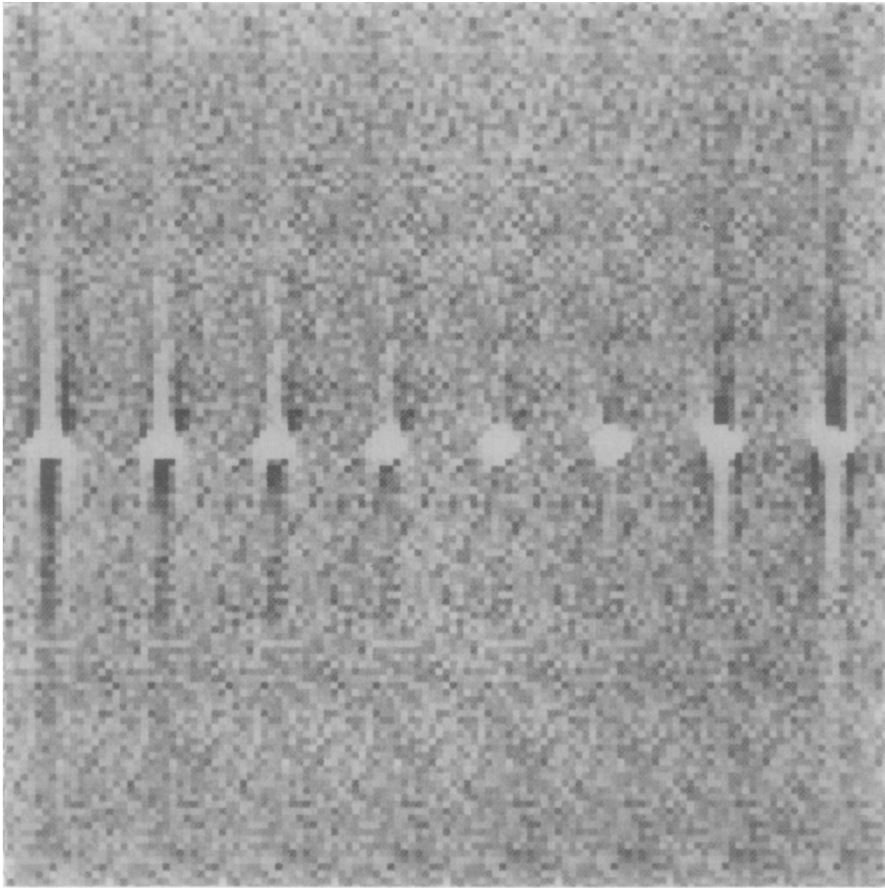

FIG. 5. Eight reconstructions of the pin of Fig. 2 from the same data using eight different values of the centering parameter in (3). The rays have been uniformly shifted to the right by the respective amounts (in millimeters) -0.2, -0.1, -0.05, 0, 0.05, 0.1, 0.2, and 0.3 from the left. The picture shows that tomography is sensitive to small (0.05 mm) errors in recentering the graticule after each translation stop, and that these errors can be measured and corrected. This corresponds to Run 1B of Table 1. For Run 1A an essentially identical picture was obtained.

scanning) is shown in the Appendix to be given by the crude approximate formula

$$f^*(x_0, y_0 + y) = \frac{2}{\pi} \frac{\delta D}{y}, \qquad b < |y|. \tag{4}$$

For example, if $D = 1000$ output units for the pin corresponding to twice the density of bone, $b = 3$ mm, $\delta = 0.05$ mm, $y = 5$ mm, the error is about 6 units, enough to show an artifact. In each of the runs of Table 1 the results agree qualitatively with (4) and exhibit the reversal of the error predicted by (4) as δ or y changes sign. If a centering correction (3) with $\delta_j = \Delta$ is used in the algorithm, (4) is of course modified by replacing δ in (4) by $\delta - \Delta$. In Fig. 5 we see that the error reverses as $\delta - \Delta$ changes sign, and this holds for the other cases of Table 1 as well. Note that (4) predicts that the error above the pin will appear as an object denser than the surrounding water, as it does in Fig. 5 when $\Delta = 0$.

In comparing Figs. 2 and 5 the artifact appears reversed, which is due to our considering the data collected with a different direction of rotation. This reversal is consistent and should be ignored.

If one considers the reconstruction as a sum of filtered backprojections where in each direction the filtered backprojection is as in (A2) of [1], which is a positive constant in the shadow of the circle and is negative outside, then the superposition of the δ-displaced backprojections is intuitively seen to give a positive error (for $\delta > 0$) above the circle and a negative error below it. The argument in the Appendix makes this more quantitative. We also show that the error in the region on either side of the circle is much smaller, of order δ^2, as would be the case with uniformly displaced rays with 360° scanning.

APPENDIX: DERIVATION OF APPROXIMATION (4)

We assume that the pin of radius b and density D is centered at the origin (as far as our approximations go, centering at the origin is not a loss of generality). Suppose that each projection is shifted by the same amount $\delta(\theta) = \delta$ in (1), $0 \leq \theta \leq \pi$, and no correction (i.e., $\delta_j \equiv 0$) is used in (3). Then the value at the point $(0, y)$ with $|y| > b$ should be zero, but is given by (3), and may be approximated by the limiting integral form of (3),

$$f^*(x, y) \doteq \frac{1}{2\pi} \int_0^\pi d\theta \int_{-\infty}^\infty P(t - \delta, \theta) \varphi(x \cos \theta + y \sin \theta - t) dt. \tag{5}$$

For weight functions φ of the type appropriate to reconstruction from projections (i.e., those whose Fourier transform $\hat{\varphi}(\omega) \doteq |\omega|$, for low frequencies ω) the inner integral in (5) is given approximately by (A2) of Appendix 1 of [1], as $\bar{Q}$ is the derivative of the Hilbert transform of P, and so

$$f^*(x, y) \doteq \frac{D}{2\pi} \int_0^\pi d\theta \bar{Q}(x \cos \theta + y \sin \theta - \delta)$$

$$= 1 - \frac{1}{\pi} \int_0^\pi d\alpha \frac{|\tau - \delta|}{((\tau - \delta)^2 - b^2)^{\frac{1}{2}}} \chi, \qquad \tau = x \cos \alpha + y \sin \alpha, \tag{6}$$

where χ indicates that the integral is carried out only over those α for which the square root makes sense as a real number, i.e., $|\tau - \delta| > b$. Here, from (A2) of [1] (with a misprint corrected), we have used

$$
\begin{aligned}
\bar{Q}(\tau) &= 2, & |\tau| &\leq a, \\
&= 2 - 2|\tau|(\tau^2 - a^2)^{-\frac{1}{2}}, & |\tau| &> a.
\end{aligned}
$$

Suppose $x = 0$, $|\delta| < b$, and $b + |\delta| < |y|$. Then it is easy to see, setting $\alpha = \beta + \pi/2$ in (6), that

$$(1/D)f^*(0, y) \doteq 1 - F(\delta/y), \tag{7}$$

where, letting $\xi = |b/y|$,

$$F(u) = \frac{2}{\pi} \int_0^{\beta_0} d\beta \, \frac{\cos \beta - u}{((\cos \beta - u)^2 - \xi^2)^{\frac{1}{2}}}, \qquad 0 \leq \beta_0 = \cos^{-1}(u + \xi) < \frac{\pi}{2}, \tag{8}$$

since the last integral in (6) is over an interval in α symmetric about $\alpha = \pi/2$. Changing variables, $\cos \beta - u = t$, we have

$$F(u) = \frac{2}{\pi} \int_\xi^{1-u} \frac{t \, dt}{(t^2 - \xi^2)^{\frac{1}{2}}(1 - (t + u)^2)^{\frac{1}{2}}}. \tag{9}$$

Since for all ξ, it is easy to see that

$$\frac{2}{\pi} \int_\xi^1 \frac{t \, dt}{(t^2 - \xi^2)^{\frac{1}{2}}(1 - t^2)^{\frac{1}{2}}} = 1, \tag{10}$$

we see that $F(0) = 1$ and it is shown below that

$$
\begin{aligned}
F'(0) = &-\frac{2}{\pi} \frac{1}{1 - \xi^2} \\
&+ \frac{2}{\pi} \frac{\xi^2}{(1 - \xi^2)^{\frac{1}{2}}} \int_\xi^1 \frac{t \, dt}{(t^2 - \xi^2)^{\frac{1}{2}}(1 - t^2)^{\frac{1}{2}}(t(1 - \xi^2)^{\frac{1}{2}} + (t^2 - \xi^2)^{\frac{1}{2}})}, \quad (11)
\end{aligned}
$$

and that F is infinitely differentiable at zero. Since $|\delta| \ll y$ we have from (7), since $F(0) = 1$,

$$f^*(0, y) \doteq -F'(0)\frac{D\delta}{y} \doteq \frac{2}{\pi} \frac{\delta y D}{y^2 - b^2}, \tag{12}$$

which gives (4) since $b^2 \ll y^2$. In the last approximation we have used the fact that the last term in (11) is less than $\xi^2/(1 - \xi^2)$ because of (10) and that $\xi^2 = (b/y)^2$ is small compared to unity. Note: $t(1 - \xi^2)^{\frac{1}{2}} \leq t(1 - \xi^2)^{\frac{1}{2}} + (t^2 - \xi^2)^{\frac{1}{2}}$ in (10).

The argument does not require x to be exactly zero, and (7), and the other equations are valid so long as $|x| < b$, i.e., in the vertical stripe about the pin. If, however, say $y = 0$ and $|x| > b$, i.e., to the right or left of the pin we have

from (6) that (with $\xi = |b/x|$ and with the same F as in (8))

$$(1/D)f^*(x, 0) \doteq F(0) - \tfrac{1}{2}F(\delta/x) - \tfrac{1}{2}F'(-\delta/x)$$
$$\doteq \tfrac{1}{2}F''(0)(\delta/x)^2, \tag{13}$$

which, since $F''(0)$ exists, is of smaller order (δ^2) than (12) as $\delta \to 0$.

We remark that if the sampling were taken over 360° rather than 180° the error due to displacement of all rays by δ would be of order δ^2, as in (13).

We indicate how to obtain (11). Choose z in the interval $(\xi, 1 - u)$ and write from (9)

$$F(u) = \frac{2}{\pi} \int_\xi^z \frac{t\,dt}{(t^2 - \xi^2)^{\frac{1}{2}}(1 - (t + u)^2)^{\frac{1}{2}}} + \frac{2}{\pi} \int_{z+u}^1 \frac{(t - u)dt}{((t - u)^2 - \xi^2)^{\frac{1}{2}}(1 - t^2)^{\frac{1}{2}}}, \tag{14}$$

by breaking up the integral in (9) from ξ to z and from z to $1 - u$ and replacing t by $t - u$ in the second integral. It is now clear that each of the integrals in (14) is infinitely differentiable in u since there now are no singularities at the limits of integration. Differentiating we get for $u = 0$,

$$F'(0) = \frac{2}{\pi} \int_\xi^z \frac{t^2 dt}{(t^2 - \xi^2)^{\frac{1}{2}}(1 - t^2)^{\frac{3}{2}}} - \frac{2}{\pi} \frac{z}{(z^2 - \xi^2)^{\frac{1}{2}}(1 - z^2)^{\frac{1}{2}}}$$
$$+ \frac{2}{\pi} \int_z^1 \frac{t^2 dt}{(t^2 - \xi^2)^{\frac{1}{2}}(1 - t^2)^{\frac{1}{2}}}. \tag{15}$$

Since this holds for each $z \in (\xi, 1)$, let $z \to 1$ using

$$-\frac{2}{\pi} \frac{1}{(1 - \xi^2)^{\frac{1}{2}}(1 - z^2)^{\frac{1}{2}}} = -\frac{2}{\pi} \frac{1}{1 - \xi^2} - \frac{2}{\pi} \frac{1}{(1 - \xi^2)^{\frac{1}{2}}} \int_\xi^z d\left(\frac{1}{(1 - t^2)^{\frac{1}{2}}}\right). \tag{16}$$

The third term in (15) tends to zero, the second is replaceable by (16), and (11) follows by a passage to the limit.

We take this opportunity to correct some errors and misprints in [1].

1. As A. Kak kindly pointed out, the first sentence of the second paragraph of Appendix I should read:

The projections $P(t) = P(t, \theta)$ of an ellipse of density one centered at the origin and with semiaxes α, β are

$$p(t) = (2\alpha\beta/a^2)(a^2 - t^2)^{\frac{1}{2}}, \qquad |t| \le a,$$
$$= 0, \qquad\qquad\qquad |t| > a, \tag{A1}$$

where $a^2 = a^2(\theta) = \alpha^2 \cos^2 \theta + \beta^2 \sin^2 \theta$ and a is the half-width of the projection in direction θ.

2. The factor $\alpha\beta/a^2$ is also missing in (A2) and (A9). Note that this constant factor makes no difference in the conclusions of [1] and was not omitted in the simulations discussed in [1, 2]. For a circle, $\alpha = \beta = a$, as in the present paper, the missing factor is unity.

3. (A8) has a parenthesis missing in $f_\varphi(x, y)$.

4. (A16) should read:

$$Q = -(2/\lambda\mu_w) \log (D/E) - 2. \tag{A16}$$

5. The line above (A16) should have "emitted" photons instead of omitted photons.

6. The referee kindly pointed out that (A2) of [1] should read:

$$\bar{Q}(t) = 2, \qquad\qquad\qquad |t| \le a,$$
$$= 2 - |t|(t^2 - a^2)^{-\frac{1}{2}}, \qquad |t| > a.$$

ACKNOWLEDGMENT

REFERENCES

1. L. A. Shepp and B. F. Logan, The Fourier reconstruction of a head section, *IEEE Trans. Nucl. Sci.* **NS-21**, 1974, 21–43.

2. L. A. Shepp and J. A. Stein, Simulated reconstruction artifacts in computerized X-ray tomography, in *Proceedings of the Workshop on Reconstruction Tomography in Diagnostic Radiology and Nuclear Medicine, April 1975* (M. Ter-Pogossian *et al.*, Eds.), pp. 33–48. University Park Press, Baltimore, Md., 1977.

3. E. C. McCullough, H. L. Baker, Jr., O. W. Houser, *et al.*, An evaluation of the quantitative and radiation features of a scanning X-ray transverse axial tomograph: The EMI scanner, *Radiology* **3**, 1974, 709–715.

4. EMI "Artifacts" booklet.